


Processing advances in liquid crystal elastomers provide a path to biomedical applications

Cite as: J. Appl. Phys. **128**, 140901 (2020); doi: [10.1063/5.0021143](https://doi.org/10.1063/5.0021143)

Submitted: 7 July 2020 · Accepted: 24 September 2020 ·

Published Online: 8 October 2020



Cedric P. Ambulo,¹ Seelay Tasmim,^{1,2} Suitu Wang,^{1,3} Mustafa K. Abdelrahman,^{1,3} Philippe E. Zimmern,⁴ and Taylor H. Ware^{1,2,3,a)} 

AFFILIATIONS

¹Department of Bioengineering, The University of Texas at Dallas, Richardson, Texas 75080, USA

²Department of Biomedical Engineering, Texas A&M University, College Station, Texas 77843, USA

³Department of Materials Science and Engineering, Texas A&M University, College Station, Texas 77843, USA

⁴Department of Urology, University of Texas Southwestern Medical Center, Dallas, Texas 75390, USA

^{a)}Author to whom correspondence should be addressed: taylor.ware@tamuedu

ABSTRACT

Liquid crystal elastomers (LCEs) are a class of stimuli-responsive polymers that undergo reversible shape-change in response to environmental changes. The shape change of LCEs can be programmed during processing by orienting the liquid crystal phase prior to crosslinking. The suite of processing techniques that has been developed has resulted in a myriad of LCEs with different shape-changing behavior and mechanical properties. Aligning LCEs via mechanical straining yields large uniaxial actuators capable of a moderate force output. Magnetic fields are utilized to control the alignment within LCE microstructures. The generation of out-of-plane deformations such as bending, twisting, and coning is enabled by surface alignment techniques within thin films. 4D printing processes have emerged that enable the fabrication of centimeter-scale, 3D LCE structures with a complex alignment. The processing technique also determines, to a large extent, the potential applications of the LCE. For example, 4D printing enables the fabrication of LCE actuators capable of replicating the forces generated by human muscles. Employing surface alignment techniques, LCE films can be designed for use as coatings or as substrates for stretchable electronics. The growth of new processes and strategies opens and strengthens the path for LCEs to be applicable within biomedical device designs.

Published under license by AIP Publishing. <https://doi.org/10.1063/5.0021143>

I. BACKGROUND

Many organic molecules are known to exhibit phases with varying degrees of orientational and/or positional order while maintaining fluidity, known as liquid crystalline phases. Mesogens, or rod-like molecules, can be designed to order into the nematic phase, a 1D ordered fluid. The nematic phase can be aligned with electric and magnetic fields, mechanical deformation, and topographic and chemical surface interactions, resulting in macroscopically anisotropic fluids that are useful in a number of applications.¹ On heating or dilution, these ordered liquids melt into a disordered, isotropic phase. de Gennes predicted that if a polymer network exhibited the nematic phase, the resulting anisotropic material would undergo reversible shape-change (actuation) triggered by order-disorder transitions.² His work led to the field of stimuli-responsive liquid crystal elastomers (LCEs).

Polymer systems exhibiting a liquid crystalline phase are typically categorized by thermomechanical properties. Liquid crystal

polymers (LCPs) are typically engineering thermoplastics. Liquid crystal polymer networks (LCNs) exhibit moderate or high crosslink density and undergo relatively small dimensional changes on heating (<10%). For the scope of this Perspective, we define LCEs as liquid crystalline polymer networks with a low crosslink density that undergo dimensional changes of >10% on heating. The reversible shape change of LCEs is dependent on both liquid crystalline phase transitions and the network structure of the elastomer.³ The orientation of the shape change is controlled through a two-step process. First, the liquid crystalline precursors, below the nematic-to-isotropic temperature (T_{NI}), are oriented in a preferential direction. Then, the material is then crosslinked to lock-in the alignment. The transition between order and disorder translates to macroscopic, reversible shape-change. For example, a uniaxially aligned LCE will contract along the director orientation and expand in the orthogonal directions. Removal of the stimulus yields a transition back to the nematic phase and a return to the initial

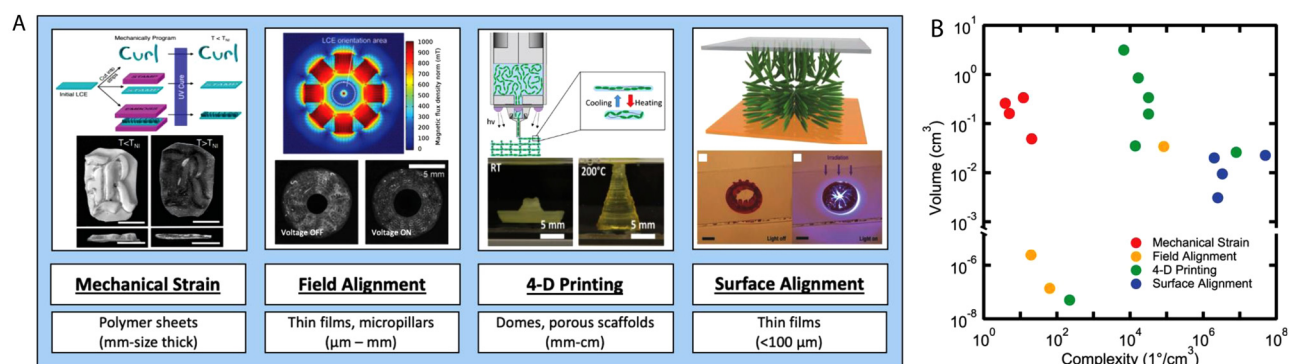


FIG. 1. (a) The table describes the different processing strategies for LCEs. Mechanical straining: schematic describing different mechanical programming methods to achieve shape-change. An embossed LCE example displacing the Rice University logo below T_{NI} and flat above T_{NI} . Reproduced with permission from Barnes and Verduzco, *Soft Matter* **15**, 870 (2019). Copyright 2019 The Royal Society of Chemistry. Field alignment: the magnetic field orientation used to align the LCE iris. Snapshot images of the LCE iris activated with voltage. Reproduced with permission from Schuhladen *et al.*, *Adv. Mater.* **26**, 7247 (2014). Copyright 2014, Wiley. Reproduced with permission from Ambulo *et al.*, *ACS Appl. Mater. Interfaces* **9**, 37332 (2017). 4D printing: 4D printing schematic of three-dimensional LCE structures. Snapshot images of combined Gaussian curvatures actuated through ambient heating. Copyright 2017 American Chemical Society. Surface alignment: schematic of the LC molecules oriented based on the surface aligned cells. Snapshot images of the aligned LCE sample folding and unfolding with irradiation of 470 nm light. Reproduced with permission from Zeng *et al.*, *Adv. Mater.* **29**, 1701814 (2017). Copyright 2017 Wiley. (b) The log-log plot describes the relationship between the volume and complexity achieved with different processing LCE strategies. The volume is defined as the largest volume fabricated within the articles. Complexity is calculated by the volume resolution that can exhibit a distinct director orientation.

form due to the crosslinks within the elastomer network. Various processing techniques have been developed that allow for the synthesis of polymer networks with a controlled network structure including alignment of the liquid crystalline phase.^{4–7}

The chosen alignment dictates and influences both the size of the material and the shape change achieved (Fig. 1). The processing must also occur during synthesis. As a result, the processing conditions of the material are inextricably linked to both the synthetic procedure and the ultimate application of the material. We explore how LCEs are aligned and fabricated, and the relative benefits of each process. LCEs aligned mechanically generate uniaxial shape changes in large samples.^{4,8,9} Magnetic alignment can be used to orient monodomains in 3D microstructures.^{5,10} Surface alignment techniques enable patterning of a complex director alignment within films, resulting in two-dimensional, thin films that morph into three-dimensional configurations.^{6,11,12} Additive manufacturing processes enable complex alignment to be built-in large-scale (cm-size) LCE actuators.^{7,13,14} In Fig. 1(a), we overview these alignment process.^{7,12,15,16} Figure 1(b) plots the volume and complexity of realized LCEs fabricated with different processing techniques.^{5–7,11–14,16–27} The volume is defined as the largest volume fabricated within each publication. Complexity is calculated by the volume resolution that defines a distinct director orientation ($Complexity = \frac{1}{resolution\ of\ director\ pattern}$). In one example of surface aligned LCEs, the director orientation can be controlled at volumes of $100 \times 100 \times 50 \mu\text{m}^3$ yielding a complexity value of $2\,000\,000\ \text{cm}^{-3}$.⁶ Comparatively, an example of mechanically aligned LCEs can be made with a single director orientation over a volume of $1 \times 2 \times 0.1\ \text{cm}^3$. This yields a complexity of $5\ \text{cm}^{-3}$.⁴ In the absence of context, the importance of the work cannot be assessed directly with volume or complexity. Throughout the review, we describe potential applications requiring large or small

actuators with uniform or intricately programmed shape change. We focus on the use of these materials as orthopedic devices, substrates for bioelectronics, scaffolds for tissue engineering, and artificial muscles. We conclude the Perspective by suggesting that LCE artificial muscles offer promise in devices for the treatment of stress urinary incontinence.

II. RECENT PROCESSING ADVANCES

A. Mechanical alignment

Mechanical forces applied to partially crosslinked LCEs induce orientation of the liquid crystalline phase; this orientation is then trapped with further crosslinking. In 1984, Finkelmann *et al.* used this approach to create an LCE where a lightly crosslinked polymer network was first synthesized by mixing polyhydrosiloxane, mono-vinyl LC monomers, and bi-vinyl crosslinkers together with a platinum catalyst and a solvent.²⁸ After gelation, and before the reaction was completed, the lightly crosslinked network can be stretched by a mechanical load. This deformation exceeded the threshold stress to induce alignment orientation and was then further crosslinked to lock the alignment. In the years that followed this seminal work, this basic method was implemented to fabricate aligned LCEs capable of reversible actuation from a variety of chemistries.^{8,29,30} Mechanical alignment is a facile process to orient relatively large samples, millimeter or centimeter scale. The large, uniaxially aligned LCEs can be exploited as artificial muscles capable of producing moderate work. For example, Yakacki *et al.* demonstrated thiol-ene LCEs capable of producing a work output of up to $295\ \text{kJ}/\text{m}^3$,¹⁷ and Yang *et al.* introduced interpenetrating polymer networks within LCEs to increase the work output to $1267\ \text{kJ}/\text{m}^3$.³¹ However, for applications requiring complex alignment or microscale samples, this process can be limiting. The limitation is

based on the difficulty of spatially varying the direction of deformation in a partially crosslinked elastomer. Over the last several years, there have been efforts to use or improve upon this alignment method to create LCEs.

The initial hydrosilation chemistry consists of only a single reaction, and as such, the processing technique relies on straining of the polymer gel during the crosslinking reaction. A key area of advance has been temporal control of the crosslinking reactions. Reaction schemes that are capable of decoupling the crosslinking reaction during the alignment step enable further alignment control. In 2015, thiol-ene chemistries emerged as a powerful approach to synthesize LCEs using controlled reactions from readily available precursors.⁴ For example, diacrylate mesogens and di-functional and tetra-functional thiols can be polymerized to create a polydomain sample through thiol-acrylate Michael addition. Under tension, the LCEs orient into monodomains and are then crosslinked through photopolymerization of excess acrylate groups [Fig. 2(a)]. The key benefit of this chemistry is that the final crosslinking is triggered via light, while the initial crosslinking proceeds thermally. The orthogonal nature of these reactions enables repeatable and facile programming of monodomains. Furthermore, spatiotemporal control of the final photopolymerization step can be used to mechanically deform a single sample to have multiple domains within a 3D form.¹⁵ The resulting actuators have a global

shape change that can be programmed beyond uniaxial shape change by either designing the director pattern or by molding the polydomain film to a complex form.

Dynamic covalent bonds within an LCE allow the alignment to be changed post-processing. All previously mentioned LCEs have permanent crosslinked networks, which means that the alignment is set during crosslinking and cannot be altered after processing. Initial LCEs with dynamic covalent bonds were polyesters, where the transesterification reaction proceeds readily above the “vitrification temperature” (T_v) which was higher than T_{NI} .³² As such, the material can be realigned above T_v and used as a shape-changing material below T_v . However, one drawback of using transesterification is that the alignment may not be stable over time as bond exchange can occur slowly during the heat activation required for shape change.²⁷ As a result, actuation strain may decrease with increasing heating time. Allyl sulfide functionalities can also be used to introduce exchangeable bonds within an LCE [Fig. 2(b)]. Allyl sulfides rearrange in the presence of free radicals which can be generated by the photoactivation of typical radical initiators. As these networks are more stable during heating, excellent repeatability of actuation strain is observed.¹⁹ However, in each of these materials, shape change is driven by ambient heating, which is difficult to employ in most applications.

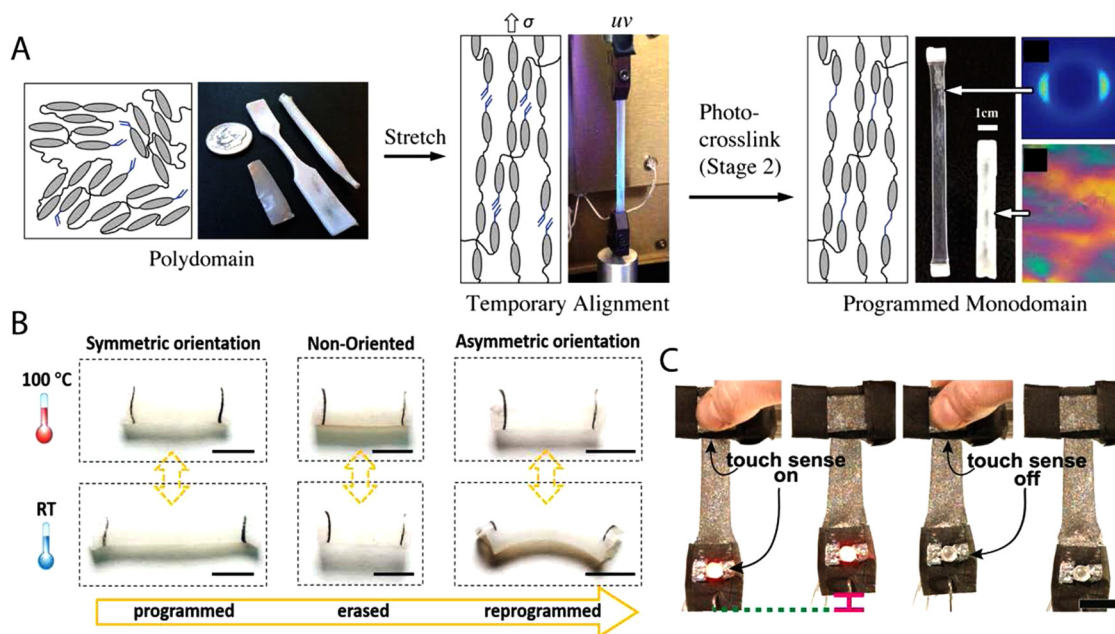


FIG. 2. (a) Illustration of the synthesis of mechanically aligned LCEs. Representative polydomain samples with different geometries are mechanically stretched into a temporary monodomain state. A photopolymerization reaction is used to establish crosslinks between the excess acrylate groups, stabilizing the monodomain of the sample. Reproduced with permission from Yakacki *et al.*, RSC Adv. **5**, 18997 (2015). Copyright 2015 The Royal Society of Chemistry. (b) Erasing the autonomous elongation and reprogramming the tube into bending actuation for a new purpose. Scale bar: 5 mm. Reproduced with permission from Qian *et al.*, Adv. Mater. **30**, 1801103 (2018). Copyright 2018 Wiley. (c) Photographs of a multifunctional architecture. LM-LCE composites function as a conductive wire to run current through an LED, as a transducer to sense touch, and as a Joule-heated actuator to lift a weight. An LED turns on when the sensing composite responds to touch, and internal Joule-heated actuation is activated. Scale bar: 1. Reproduced with permission from Ford *et al.*, Proc. Natl. Acad. Sci. U.S.A. **116**, 21438 (2019). Copyright 2019 National Academy of Sciences.

Mechanical alignment is an efficient and the primary method used to orient LCE-composites. The introduction of composite fillers allows for the design of LCEs that respond to a variety of stimuli, which may enable the use of LCEs in applications where ambient heating is impractical. Typically, LCE composites are designed to enable photothermal absorption or electrical conductivity. The processes to disperse microscale and nanoscale fillers in polymer precursors often involve solvents. Mechanical alignment occurs after gelation and removal of the solvent, which decouples particle dispersion and the alignment process. The processing of electrically conductive LCEs is particularly aided by the processing freedom associated with mechanical alignment, as the large volume fraction of particles needed for percolation often disrupts other LC alignment techniques. For example, Joule heating can be used to induce shape-change in LCEs by combining carbon black (2 wt. %) or liquid metal droplets (50 vol. %) in the LCE matrix [Fig. 2(c)].^{33,34} Carbon nanotubes, which are difficult to disperse at high loadings without solvents, can be used to create IR responsive or multi-responsive materials.^{35–37} Mechanical alignment is a versatile process which can be coupled with other strategies to make aligned composites, such as surface coating of conductive or absorptive materials.^{38,39}

The variety of LCE chemistries amenable to mechanical alignment strategies enables materials with a wide range of properties to be synthesized. For example, a family of thiol-ene/acrylate chemistries can be used to tune T_{NI} of these main-chain LCEs from 58 to 113 °C by altering the functionality of crosslinkers or the amount of excess acrylate groups.^{17,26} This wide control is somewhat uncommon in other classes of LCEs and can partially be attributed to the versatility of the mechanical programming method. Interestingly for biomedical applications, some versions of this material chemistry were found to be non-cytotoxic before and after the final crosslinking. This biocompatibility coupled with tunable T_{NI} 's represents an important step toward applying LCEs in the biomedical field.

In summary, the processing freedom of mechanical alignment of LCEs allows for their application to a wide range of material chemistries. As a result, mechanical alignment has been used to synthesize side-chain LCEs, main-chain LCEs, LCE composites, and LCEs with dynamic covalent bonds. However, the complexity of shape-change, achievable alignment, and control within the microstructure is limited due to the loading conditions that can be induced. Therefore, strategies enabling complex alignment and control over small-size scale LCEs are necessary.

B. Field alignment

Magnetic and electric fields can be used to direct the molecular orientation of LCEs. Mesogenic monomer solutions with anisotropic diamagnetic or dielectric properties orient themselves in the presence of a magnetic or electric field of sufficient strength.^{16,40} A key distinction between field alignment and mechanical alignment is that these fields are best suited to orient relatively low viscosity monomers and not crosslinked gels. After orientation, these monomers can be polymerized to yield oriented LCEs.

A key advantage of magnetic orientation is that it can be readily combined with soft lithography such that many microscale,

oriented LCEs can be fabricated.⁴¹ For example, microposts have been fabricated through a one-step photopolymerization of mesogenic monoacrylates with diacrylate crosslinkers after being initially aligned in a magnetic field. This synthetic approach is well-suited to the alignment technique as the low viscosity of the LCE precursors allows for both magnetic alignment and soft-lithography. Additionally, acrylate monomers can be readily copolymerized leading to tunable mechanical properties. For example, the alteration of the mesogenic diacrylate monomer from side-chain to main-chain increases the thermally induced shape change from 40% to 400%.^{10,42} Though high actuation strain values were achieved, these microactuators are limited to uniaxial contractions and expansions.

More complex shape change within microstructures is achieved by offsetting the orientation of the magnetic field from the geometric axes of the microstructure.⁵ For example, microposts can be programmed to either bend, twist, shrink, or expand by varying the offset angle between the magnetic field and the long axis of the microposts. As the magnetic field directly aligns the LC monomers, this methodology can be expanded to a range of microstructures. For example, honeycomb structures can be designed to buckle, shear, and transform into a brick-wall geometry [Fig. 3(a)]. Furthermore, imposing a magnetic field with a spatial gradient during polymerization enables area specific deformations within an LCE microstructure array [Fig. 3(b)]. This allows for microstructures within a single array to deform in various controlled ways depending on the complex orientation of the magnetic field during crosslinking [Fig. 3(c)].⁴³ To allow for simultaneous bending and twisting within a single microstructure, processes are needed that result in controllable multi-domain alignment within a microstructure. Modeling of multi-domain microstructure actuation has been simulated; however, experimental results are yet to be achieved.⁴³ We imagine applications for microstructures that undergo complex shape changes in a variety of fields. In medical applications, active microstructures may enable dynamic adhesives⁴⁴ or actuators at the size scale of living cells.^{45,46}

C. Surface alignment techniques

Unlike mechanical stress or electromagnetic fields, surface alignment allows for a voxel by voxel programmable alignment of LCEs. Surface alignment techniques exploit the susceptibility of liquid crystals to form nicely ordered monodomains on oriented surfaces in order to minimize surface energy.^{47–50} When an LCE precursor is filled within a pre-programmed cell, mesogens orient along the programmed direction through a phenomenon known as surface anchoring. Furthermore, the programmed orientation propagates throughout adjacent layers due to the misalignment energy penalty. Programming of substrates can be accomplished by rubbing polymer coated substrates, aligning photosensitive molecules with polarized light, or by patterning topographical features with lithography (Fig. 4).^{11,51–55} Critical to the formulation of surface alignable LCEs is the formulation of a low viscosity nematic monomer solution. This approach is modeled after the pioneering work on creating oriented liquid crystal polymer networks from nematic diacrylates in 1991.⁵⁶ The key distinction of LCEs from these LCNs is that chain extension reaction and crosslinking

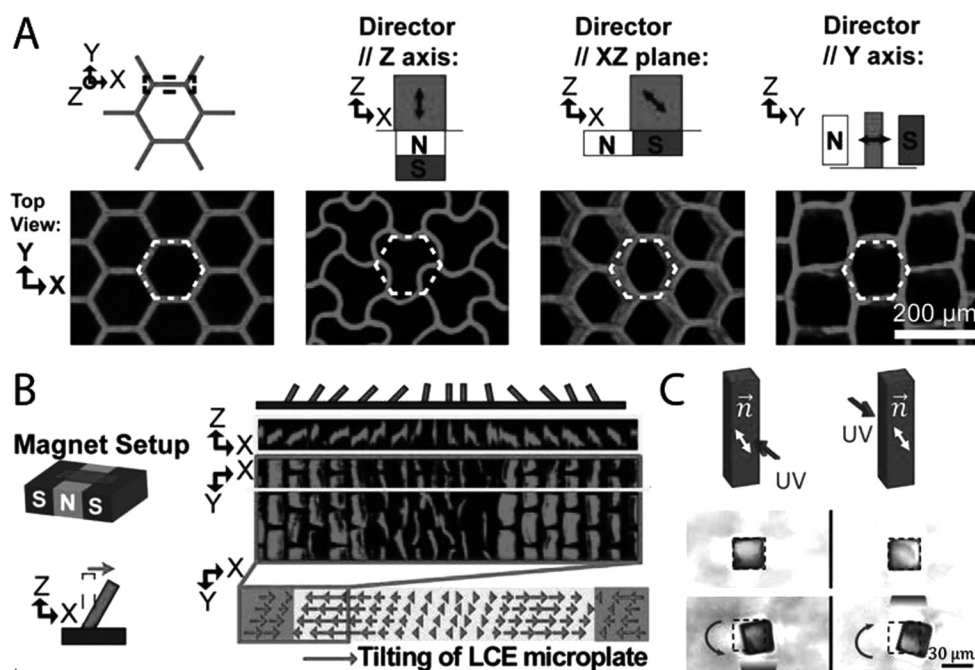


FIG. 3. (a) Confocal images of undeformed and deformed honeycomb structures. Deformation of honeycomb structures is determined by the orientation of the nematic director, as illustrated by the double-headed black arrows. White lines indicate the structure before deformation. Reproduced with permission from Yao *et al.*, Proc. Natl. Acad. Sci. U.S.A. **115**, 12950 (2018). Copyright 2018 National Academy of Sciences. (b) Fabrication of array of microstructures. Confocal images of microstructures demonstrating actuation toward the center caused by the spatial gradient in the molecular orientation due to the magnetic setup before crosslinking. Reproduced with permission from Yao *et al.*, Proc. Natl. Acad. Sci. U.S.A. **115**, 12950 (2018). Copyright 2018 National Academy of Sciences. (c) Magnetically aligned LCE microstructures demonstrating bending toward the light. Double headed black arrows demonstrate the nematic direction, while single arrow purple lines illustrate the area of the incident UV light. Reprinted from Waters *et al.*, Sci. Adv. **6**, eaay5349 (2020). Copyright 2020 American Association for the Advancement of Science, distributed under a Creative Commons Attribution NonCommercial License 4.0 (CC BY-NC).

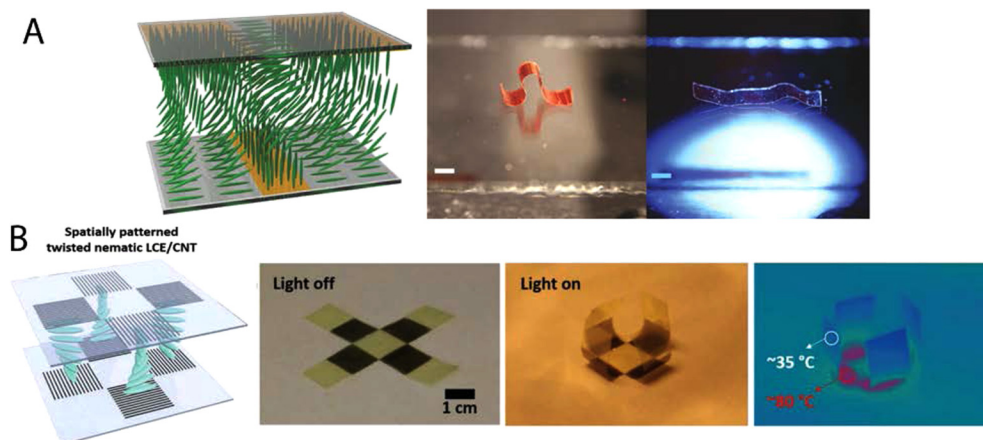


FIG. 4. (a) Schematic illustrating molecular orientation of LCE transitioning from nematic to homeotropic along the plane and nematic to homeotropic orthogonal to the plane. This causes a photothermally induced crawling actuation in the presence of light. Scale bar: 2 mm. Reproduced with permission from Zeng *et al.*, Macromol. Rapid Commun. **39**, 1700224 (2018). Copyright 2018 Wiley. (b) Schematic illustrating twist alignment through the thickness of an LCE cell caused by the orientation of the carbon nanotube forest. This orientation allows for a photothermally induced bending actuation. Reproduced with permission from Kim *et al.*, Adv. Funct. Mater. **29**, 1905063 (2019). Copyright 2019 Wiley.

reactions are required to yield the low crosslink density necessary for LCEs. Critically, each reaction step that builds molecular weight must occur in the nematic phase, which limits the use of solvents. Both step-growth reaction schemes, such as thiol-ene or thiol-Michael addition reactions,⁵⁷ and chain-growth reaction schemes, like radical acrylate polymerization⁵⁸ and cationic epoxide polymerization,⁵⁹ have proven compatible with developing surface aligned LCE films.

Surface alignment can be used to process LCEs where chain extending and crosslinking strategies are performed in the nematic phase. A two-step synthesis was developed in 2015, where nematic diacrylate monomers are first chain extended with n-butylamine through a step-growth Michael addition reaction within an aligned cell.⁶ A laser was used to align the photosensitive molecules on the cell spot by spot, allowing for the variation of the molecular orientation at a resolution of $100 \times 100 \mu\text{m}^2$, before LC inclusion. The oligomers that are formed remain in the nematic phase, follow the orientation of the cell, and are then crosslinked by radical photopolymerization of the acrylic end groups. Using this approach, actuators that fold, twist, and stretch have been produced. Furthermore, photolithography techniques can be exploited to pattern microgrooves to spatially control the orientation of LCEs with single-micrometer resolution.¹¹ We note that each of the reported surface aligned LCEs currently require high temperatures to induce shape change. A chemical strategy to increase the number of methylene groups of alkyl side chains in nematic LCEs results in lowering T_{NI} from 102 to 79 °C, allowing for additional control over processing and actuation conditions.⁶⁰ Additionally, surfaced aligned LCEs can be formulated to contain light-responsive molecules, enabling photothermally or photochemically driven shape changes.^{12,61-64} The ability to control transition temperatures coupled with diverse actuation stimuli is important for the eventual applications of this material. Surface alignment strategies enable high resolution control of director patterning as compared to other alignment strategies. This control of LCE microstructure can be taken advantage by applications that utilize films with specific and controlled shape-change.

D. 4D printing

4D printing describes the process of fabricating three-dimensional structures that change shape over time, the fourth dimension. Shape memory polymers can be printed using stereolithography to create structures that can be deformed into a new shape and then triggered to return to their original configuration.⁶⁵⁻⁶⁷ Strategies to program the stimulus-response during printing provide more control over the shape-morphing response. Direct-ink write (DIW) printed hydrogel composites are designed to orient microstructures during printing, resulting in objects that swell anisotropically as dictated by the print path.⁶⁸ The key to these strategies is programming the stimulus-response within the microstructure to manipulate macroscopic shape-change. Several techniques have been developed to orient LCE precursors during printing enabling a powerful set of 4D printing strategies. The ability to control actuation response within cm-scale LCE actuators is an important step toward artificial muscle applications.

Two-photon polymerization allows for the fabrication of microscale LCEs with a controlled structure.²² This technique uses a layer-by-layer process, where an IR laser directs spatial crosslinking within the X-Y plane of one layer and then shifts upward to the next layer. Prior to crosslinking, the acrylate-functionalized liquid crystalline monomer solutions are aligned by an underlying patterned substrate. The resolution of this technique allows for the generation of features with a width of 300 nm. Unlike LCEs formed from surface alignment strategies in cells, true 3D structures can be realized such as porous LCEs with a controlled alignment [Fig. 5(a)]. Since the alignment is dictated by the surface energy of the underlying substrate, the alignment within the microstructure is uniform and noncomplex.

DIW printing is used to program the stimulus-response in cm-scale LCEs.^{7,13,14} To create DIW-printable LCEs, inks must be formulated such that extrusion induces alignment of the ink which is then trapped into a 3D solid. Acrylate-terminated nematic oligomers that are suitable for printing can be synthesized by aza-Michael addition between a nematic diacrylate and a primary amine. The director orientation is controlled through the extrusion print path within the X, Y, and Z planes. Similar to prior LCE alignment techniques, printing needs to occur below T_{NI} with subsequent crosslinking to lock-in the director profile. The control over the print path allows director complexity, normally associated with surface alignment methods, to be spanned to cm-size, 3D structures with porosity and Gaussian curvature [Fig. 5(b)]. The coupling of 3D geometries with complex patterning can lead to emergent shape-morphing properties. Porous structures are capable of dramatically shrinking in volume on heating, even though the intrinsic material deformation is isochoric. A composite focusing lens comprised of a 4D printed LCE “o-ring” and PDMS lens undergoes changes in lens power upon heating [Fig. 5(c)].¹³ Additionally, the ability to generate concentric patterns onto curved structures can help amplify the power of inherently low elastic modulus LCEs. Locally programming orientation on a 3D curved surface was not feasible through previous alignment techniques. Hemispherical shells printed with concentric patterns yield a “peaked” hemisphere upon heating as previously predicted by Warner *et al.*⁶⁹ By combining regions of positive and negative Gaussian curvatures, fast snap-through actuation under 16 ms is achieved.⁷ DIW printing further demonstrates the freedom to design geometries that can result in LCE actuation properties that have not been achieved through prior processing techniques.

DIW fabricated LCE actuators are of the appropriate scale to generate forces that can be used to manipulate the human body. However, the activation temperature for the aza-Michael addition chemistry is over 100 °C, which precludes the use of these materials in biomedical applications. Thiol-ene chemistry enables systematic control of both T_{NI} and cross-link density.^{23,70} A 2-click thiol/acrylate and thiol/ene chemistry enables LCEs with tunable T_{NI} 's ranging from 20 to 80 °C.²³ The nature of the chemistry allows for the capability to interchange the mesogens and/or thiol spacers to influence LCE properties. This freedom enables the fabrication of 4D printed LCEs capable of 20%–30% actuation strain, similar to skeletal muscle,⁷¹ below the body's threshold of pain at 50 °C.⁷² We note that LCE properties and behavior can be tuned depending on the specific application envisioned. For example, some

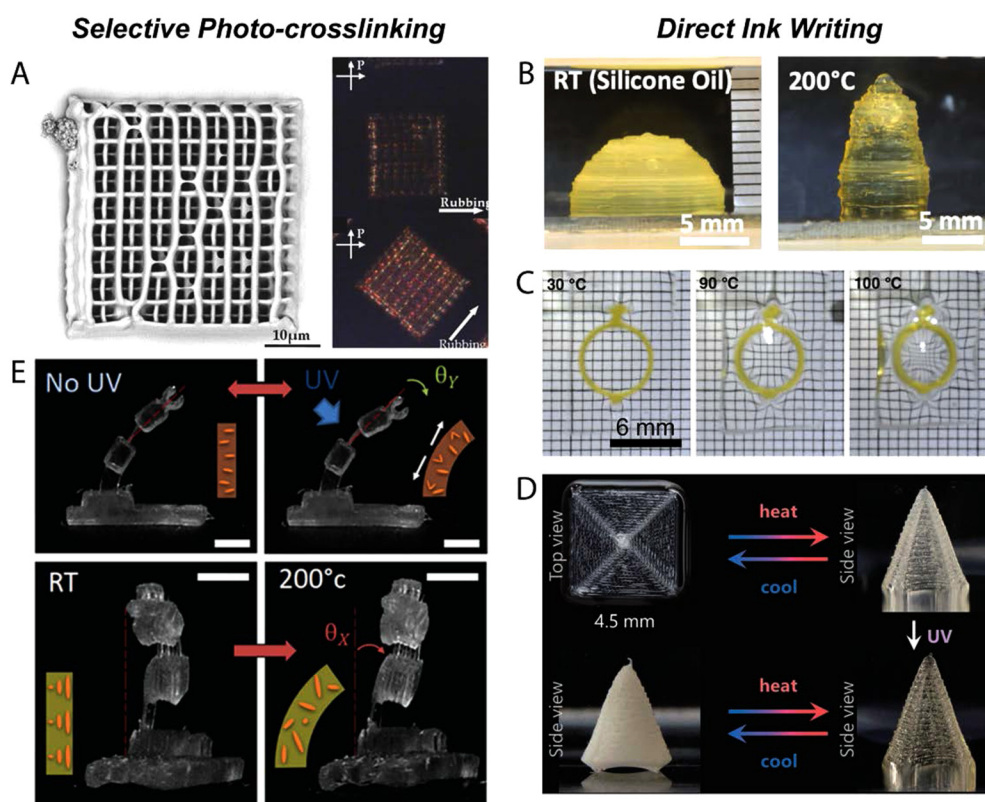


FIG. 5. (a) A two-photon polymerized porous microstructure exhibiting alignment as denoted by a change in birefringence under cross polarizers. Reproduced with permission from Zeng *et al.*, *Adv. Mater.* **26**, 2319 (2014). Copyright 2014 Wiley. (b) A DIW printed hollow dome with concentric patterning cones upon heating. Reproduced with permission from Ambulo *et al.*, *ACS Appl. Mater. Interfaces* **9**, 37332 (2017). Copyright 2017 American Chemical Society. (c) A DIW printed “o-ring” embedded in PDMS demonstrating magnification capabilities on heating. Reproduced with permission from López-Valdeolivas *et al.*, *Macromol. Rapid Commun.* **39**, 1700710 (2018). Copyright 2018 Wiley. (d) A concentric patterned square undergoes a cone shape fixation with UV light after thermal actuation. The shape is fixed due to the dynamic bonds within the LCE. Reproduced with permission from Davidson *et al.*, *Adv. Mater.* **32**, 1905682 (2020). Copyright 2020 Wiley. (e) A stereolithographic printed LCE micro-gripper exhibits small bending deformations. Scale bar: 1 mm. Reproduced with permission from Tabrizi *et al.*, *ACS Appl. Mater. Interfaces* **11**, 28236 (2019). Copyright 2019 American Chemical Society.

previously reported thiol–ene compositions can be tuned to decrease the amount of strain achieved and reduce the thermal stimulus needed. Using the tunability of this material’s chemistry and the ability to print multiple materials in a single structure, 4D printed objects can be fabricated with varying activation temperatures. Through the combination of low- and high-temperature responsive LCEs, thermal sensing is embedded within an LCE gripper that grasps an object based on temperature. Additionally, autonomous self-locomotion is demonstrated within a soft robot by combining various LCE hinges that activate at different temperatures when introduced to a heated surface.^{23,73} The addition of tunable chemistries expands the scope for 4D printed LCE actuators within human-interfacing designs.

For implantable device applications, shape-change may need to be maintained over long periods of time. For LCE actuators, this can prove problematic as the shape-change would need a constant application of stimuli. Where constant application of stimuli may not be feasible, an LCE that passively retains its actuated form may prove

successful. Using dynamic bond exchange, similar to chemistries utilized in previous alignment techniques, LCEs were fabricated to reconfigure upon heat and permanently retain that configuration via UV light.⁷⁴ The basis of the LCE ink is a 2-click thiol/acrylate and thiol/ene chemistry, but the thiol molar ratio is split 50:50 between allyl disulfide and ethylene dioxydiethane dithiols. The allyl disulfide exhibits a dynamic bond exchange property post initial crosslinking. This specific chemistry uses two photoinitiators: one for the initial crosslinking between thiol spacers and vinyl crosslinkers during printing and the other to induce dynamic bond exchange for shape fixation post-printing. This results in LCE actuators capable of shape retention with UV light after thermally induced actuation. For instance, printing a concentric square will lead to a coning actuation upon heating that can then be locked in via UV light irradiation [Fig. 5(d)]. This chemistry enables further control over the actuation response within DIW-printed LCE actuators.

DIW printing allows for the fabrication of cm-size LCEs with controllable alignment patterns; however, the alignment resolution

is limited to the nozzle size used. The nozzle size is not a fundamental limitation of the technique, but so far, the smallest nozzle diameter used to print LCEs has been $150\ \mu\text{m}$.¹³ Stereolithographic processes allow for a higher resolution printing, comparatively. Processing LCEs with this technique provides the ability to generate highly intrinsic structures voxel by voxel [Fig. 5(e)].²⁴ Similar to other resins for stereolithography, the LC precursors are low molecular weight solutions. This solution is composed of homopolymerizable diacrylate mesogens, photoinitiators, inhibitors, and light absorbers to direct specific laser patterning/crosslinking. Director patterning is induced by a controlled rotating magnetic field allowing for multiple degrees of alignment. Although the resolution of structures and alignment is increased, the use of diacrylate mesogens yields a muted shape-morphing response. This limitation and single documented chemistry currently limit stereolithographic processed LCEs in actuator applications.

4D printing processes combine the ability to control both complex director patterning and geometric parameters to fabricate LCE actuators. These revolutionary processing strategies enable cm-size, 3D LCE structures with spatially varied director patterns. The increased range of chemistries has been demonstrated to be compatible with DIW printing; as a result, LCE actuators that actuate over temperature ranges that are suitable for implementation in human-interfacing devices are feasible. Furthermore, the LCE processing techniques allow for patient-specific designs within implantable or wearable biomedical devices.

E. Other LC materials

All the aforementioned processes focus on the ability to program the shape-change of LCEs by orienting a liquid crystalline phase. However, the processes discussed here are also relevant to other materials that exhibit liquid crystalline phase behavior. Liquid crystal polymer networks, typically highly crosslinked nematics, share many of the same processing requirements as certain classes of LCEs. These materials have found use in displays^{75–78} and as dynamic coatings,^{79,80} and their relationship to LCEs has been previously reviewed in detail.⁸¹ However, a range of liquid crystal polymers (LCPs), such as Kevlar, are often aligned such that mechanical properties are maximized along the fiber axis. In addition to well-known processes such as fiber drawing and injection molding, Vectra-based LCP structures printed using DIW printing have extremely high elastic moduli due to the orientation of the LC phase during processing.⁸² Chromonic liquid crystal hydrogels can be polymerized after alignment of the lyotropic monomer solution where the liquid crystal phase controls the stimulus-response and elastic modulus of the gel.^{83,84} It is likely that the processing of LCPs and LC hydrogels will continue to evolve with processing conditions and chemistries of LCEs.

III. RECENT APPLICATION ADVANCES

Stimuli-responsive materials are often designed to function as biomaterials as the dynamic nature of these materials can be used to augment or replace the dynamic behavior of natural tissues. Target applications for LCEs are anisotropic biomaterials that dictate cellular or tissue function and biomedical devices that require reversible shape change. Different chemistries and processing techniques for

fabricating LCEs enable a myriad of tailorable properties for different applications. Here, we look into some of the ways that LCEs have been proposed for biomedical applications and use these examples to motivate thoughts on future roles for LCEs.

A. Orthopedic applications

Most load-bearing biological tissues (bones, muscles, and connective tissue) have anisotropic and heterogeneous mechanical properties, while most biomaterials are isotropic and homogeneous. LCEs may offer opportunities where material anisotropy and heterogeneity can be used to mimic the properties and functions of native tissues. For example, LCEs can be synthesized with both polydomain (PD) and monodomain (MD) regions in a single material. An intervertebral disk (IVD) model LCE, broadly consisting of regions that mimic the annulus fibrosus and the nucleus pulposus, can be fabricated using both polydomain (PD) and monodomain (MD) regions within one material [Fig. 6(a)]. The resulting material has anisotropic and elastic behavior in certain regions, while exhibiting energy-absorbing behavior in other regions. PD LCE is used to construct the nucleus pulposus central part to provide mechanical damping to intervertebral disk. Under load, many microscopic domains present in the PD region reorient.⁸⁵ This property enables PD LCEs to dissipate and absorb applied mechanical energy. The MD LCE, with a compressive modulus of 2.3 MPa, resembles the annulus fibrosus part providing structure and elasticity to this disk replacement.⁸⁶ Additional chemistries and processing techniques can further patient specificity for load-bearing applications. Semi-crystalline LCEs can be designed to have heterogeneous modulus over time, where a low modulus LCE crystallizes into a rigid structure. These materials have been proposed for intervertebral fusion cages used to separate two adjacent vertebrae. The soft elastic state is important during implantation as it enables the implant to conform to the topography of vertebrae [Fig. 6(b)]. The soft and rubbery elastomer crystallizes hours after implantation with an increase in its elastic modulus from 0.8 MPa to 80 MPa. The device shows minimal creep after 1×10^6 cycles of compressive loading, analogous to the compressive load exerted by the vertebral endplates in the body. The ability to 3D print these devices gives even more flexibility in fabricating devices customized to each patient's anatomy. These LCEs undergo minimal water absorption, leading to minimal changes in mechanical properties of the LCE on exposure to water.²⁵ Nonetheless, work remains to verify the chemical stability of these and other LCEs in simulated implanted conditions. The resulting load-bearing LCEs are largely enabled and tailored through both LCE chemistry and molecular orientation.

B. Cell culture

Control over cellular alignment and organization play an important role in tissue engineering.⁸⁷ LCEs with controlled molecular alignment may serve as tissue scaffolds that can influence cellular alignment and organization.⁸⁸ LCE coatings prepared in the smectic A phase and uniaxially oriented using surface techniques can induce cellular alignment. The LCEs form a unidirectional nanogroove topography with an average depth of around 20 nm and a period of $1\text{--}3\ \mu\text{m}$. Human dermal fibroblasts (HDFs) cultured on this substrate proliferate and follow the alignment along

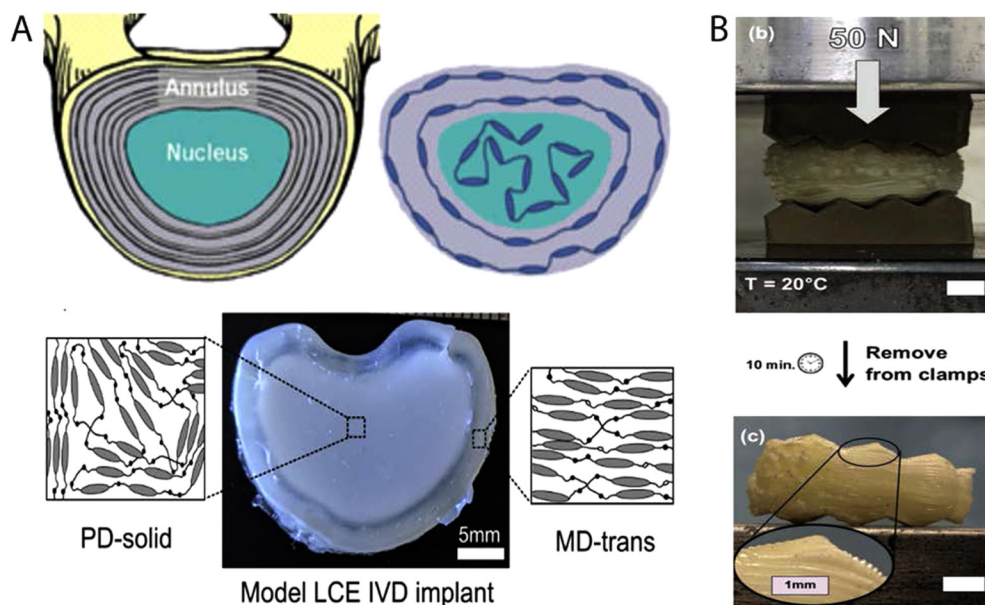


FIG. 6. (a) Schematic diagram of a model IVD designed by following the collagen alignment in the IVD with the mesogen alignment of LCE (top). IVD implant made of the LCE material where the solid polydomain LCE is used to construct the nucleus pulposus part of the implant, and transversely loaded monodomain LCE is used to construct the outer annulus fibrosus part of the implant. Reproduced with permission from Shaha *et al.*, *J. Mech. Behav. Biomed. Mater.* **107**, 103757 (2020). Copyright 2020 Elsevier. (b) 3D printed semicrystalline LCE polymer is subject to 50 N of compressive force between two platens shaped with saw tooth (top). After 10 min, the 3D printed device conforms to the topography of the platens on a large and small scale. The device keeps its new shape due to an increase in modulus after crystallization. Reproduced with permission from Volpe *et al.*, *Adv. Healthc. Mater.* **9**, 1901136 (2020). Copyright 2020 Wiley.

the nanogrooves.⁸⁹ Photoalignment techniques, on the other hand, enable fabrication of LCEs with complex topographical features [Fig. 7(a)]. The spatially patterned alignment dictates variations in cell density and phenotype.⁹⁰ This opens the door to engineering substrates that can grow cells with not only predetermined alignment but also control over their cellular organization.

In addition to orienting cells through topographic cues, the reversible shape change of LCEs can be used as a means to induce dynamic cell alignment. Many biological tissues, such as muscles, bones, and connective tissue, are subject to repeated mechanical deformation during development and normal function. Cell culture in an environment that provides stresses and strains similar to those in the body plays an important role in maintaining cell activity and phenotype.⁹¹ LCEs prepared via hydrosilation and doped with carbon black serve as substrates, where cell alignment is controlled via periodic reversible shape change.³³ CB particles are incorporated in the LCE bulk and surface to enhance the thermal conductivity of the LCE [Fig. 7(b)]. As is the case for many LCEs, the temperature required for shape change can threaten cell viability. However, in properly designed culture environments, the heat capacity of the water moderates the temperature changes observed by the cells. After cyclic actuation of the LCE substrate, primary rat cardiomyocytes can proliferate and align reaching confluence. While future research is needed to further explore the relationship between cell alignment and actuation, this work shows promise in utilizing LCEs for active 2D cell culture and cell

alignment.³³ Controlling cell alignment in 2D does not fully mimic the *in vivo* environment, thus posing a need for the development of 3D scaffolds.

3D scaffolds are better at simulating the natural cellular environment.⁹² Native tissues grow in a 3D environment and have different phenotype and morphology compared to cells grown in 2D environments.⁹³ LCEs are suitable materials for developing 3D scaffolds as LCEs are biocompatible and easily processed into porous structures.⁹⁴ Porous structures are synthesized through an emulsion polymerization of acrylate-based LCE monomers, yielding a structure made of interconnected microspheres that can be used for growing, for instance, muscle cells.⁹⁵ Additionally, scaffolds with fully interconnected microchannels can be developed by molding polycaprolactone-based LC block co-polymers within a sacrificial foam structure.⁹⁶ In one study, this scaffold does not show signs of major degradation until 15 wk, allowing considerable time for cell growth.⁹⁷ In each of these truly 3D scaffolds, alignment is challenging to explicitly control. Progress in processing strategies, like 4D printing, may enable advances where 3D LCE geometries are utilized.

C. Bioelectronics

Advances in bioelectronics are critical to creating stable interfaces between the human body and machines. Traditional electronics are flat, rigid, and fragile. By contrast, bioelectronics must

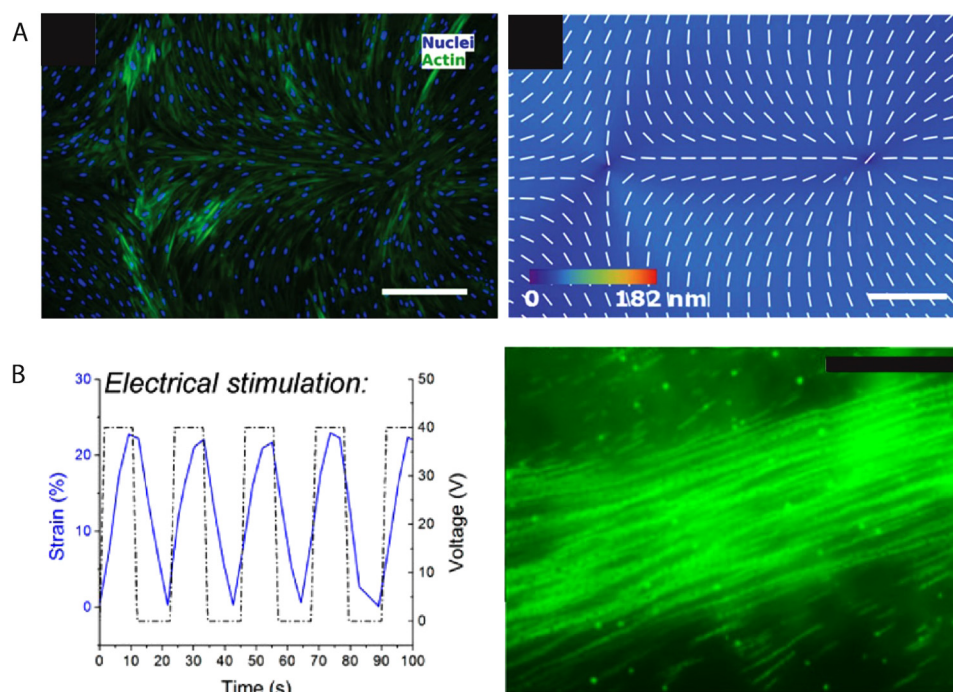


FIG. 7. (a) Fluorescently labeled HDF cells following the predetermined alignment of the substrate with a $(-1, +1)$ radial pattern (left) and PolScope image of n LCE pattern of LCE in contact with the cell growth medium (right). Scale bar: $300\ \mu\text{m}$. Reprinted from Turiv *et al.*, *Sci. Adv.* **6**, eaaz6485 (2020). Copyright 2020 American Association for the Advancement of Science, distributed under a Creative Commons Attribution NonCommercial License 4.0 (CC BY-NC). (b) Graph showing 30% strain occurring in the span of 10 s with up to 40 V power (left). Stalked fluorescent images on the right show uniaxial stretching leading to alignment. Scale bar: $50\ \mu\text{m}$. Reproduced with permission from Agarwal *et al.*, *ACS Macro Lett.* **5**, 1386 (2016). Copyright 2016 American Chemical Society.

directly interface with 3D, soft, and moving tissues. 3D and stretchable electronics can be realized through surface-aligned LCEs. As noted in Sec. II C, surface alignment techniques allow for spatial control of the director within flat films.^{6,12,47,60,61} Certain LCEs are suitable for the deposition and patterning of thin-film electronic materials due to the LCE substrate remaining laminated onto a carrier substrate during the microfabrication processing. The anisotropic elastic modulus of LCEs can be patterned such that brittle electronics are protected by localizing strain to sacrificial regions of the LCE substrate.^{98–100} Homeotropic regions within an otherwise planar aligned substrate preferentially deform irrespective of the loading axis within the plane of the substrate, enabling omnidirectional stretchability. Patterned molecular order in LCEs can also be used to control shape and extensibility in LCE-based electronics. Notably, shape varies continuously as a function of temperature on both heating and cooling. If the LCE is crosslinked at temperatures above the used temperature, cooling to the used temperature will induce a programmable shape change. Using this approach, the LCE substrate can be designed to “pop up” into a form that is stretchable or conforms to 3D tissues. For example, LCE substrates that morph from planar, during processing, to helical, post-processing, are capable of withstanding cyclical strain of at least 60% over thousands of cycles.⁹⁸ These materials are also non-cytotoxic and capable of being suitable for *in vitro* multielectrode arrays for recording the behavior of neurons in culture.⁹⁹

LCEs utilizing this processing technique hold promise as deployable, *in vivo* multielectrode arrays to record neural activity. The longevity and performance of intracortical neural interfaces are limited by the immune response. Initial reports suggest that LCEs can deploy from planar to 3D after implantation in cortical tissue.

This deployment is a strategy to move electrodes within the tissue away from the immune response associated with the bulk of the implanted device.¹⁰⁰ However, the current devices are too large to effectively evade the immune system after deployment. Although this processing strategy can fabricate fixed, 3D geometries suitable for stretchable electronics, further efforts to miniaturize these deployable electronics are needed for future neural applications.

D. Actuators

Reversible shape change is perhaps the salient feature of LCEs. The use of shape-change to perform mechanical work is the focus of many research efforts in the field. We contend that the advances made in both processing and formulation are close to enabling the use of LCEs for biomedical applications. Specifically, LCEs could prove useful where work can be reversibly done on the body as artificial muscles. While different applications will undoubtedly require a number of material formulations, we expect successful materials to (1) actuate using relatively small temperature changes, (2) heat using light or current, and (3) produce moderate stresses.

Smart materials utilized in biomedical devices must be able to achieve functionality in physiologically relative conditions. As noted in Sec. II C, most LCEs need a temperature of $>80\ ^\circ\text{C}$ to achieve actuation strains of $>10\%$ – 15% . The use of these high transition temperature LCEs would not be ideal as thermal damage would likely occur in the surrounding tissues before any useful shape-change. Chemistries utilizing thiol–ene click reactions show the capability of generating LCEs with actuation strains of 20% – 30% below $50\ ^\circ\text{C}$.^{23,70,73} LCE actuators fabricated with these chemistries can be imagined as artificial muscles. In applications where

complex shape-change is necessary, tunable 2-click thiol/acrylate and thiol/ene chemistries can generate 4D printed actuators with $\leq 25\%$ actuation strain depending on LCE formulation. This chemistry has been previously described in the 4D printing section. Although activation temperatures are capable of being tuned below the body's threshold of pain and damage, efficiently powering the LCE systems with thermal energy can prove cumbersome and difficult within a device setting.

LCE composites and systems can be designed to absorb light, exhibit electrical and thermal conductivity, or have mechanical properties that cannot be achieved with LCEs alone. These properties are critical in many applications specifically artificial muscles. Light sources and battery-powered systems are more feasible within biomedical device designs and allow for facile device control. For example, CNT-LCE composites have demonstrated the ability to absorb light and transduce light to thermal energy.^{101,102} CNT-LCEs integrated as artificial muscles in a tensegrity robot can be selectively activated using near-IR light. The locomotion path and speed are controlled by determining specific muscle activation.¹⁰² Additionally, acrylate-based, biocompatible, light-responsive LCEs are potentially suitable as cardiac contraction assist devices. These surface aligned LCEs exhibit a twitching actuation in response to light (up to 150 mW/cm^2 intensity) that can improve twitch tension levels of heart muscle from 25 mN/mm^2 to $\sim 100 \text{ mN/mm}^2$.¹⁰³ Control and specificity over multiple LCE actuators are necessary to ensure proper function within patient-interfacing designs.

LCE systems that exhibit electrical conductivity can undergo shape change by resistive heating.^{34,38,104,105} For example, LCE-CB nanocomposites overlaid with compliant Kapton-based electronics can locomote in a controlled crawling motion, inspired by the motion of inchworms [Fig. 8(a)]. To develop this robot, CB nanoparticles are doped into the LCE matrix for better thermal conductivity. This composite is then aligned through mechanical straining. The modulus mismatch between the LCE and Kapton film leads to bending of the LCE during actuation.³⁸ Additionally, tubular LCE actuators are fabricated by sandwiching multiple separate heating wires between LCE films. Activating specific heaters in the LCE robot allows for selective actuation configurations enabling the LCE to be used as soft robots or grabber.¹⁰⁵ Such robots show promise in many areas such as surgery and rehabilitation. However, heat is delivered by inextensible electronics which limits the ability to program shape transformations. A Joule-heat responsive composite is fabricated by embedding liquid metal (LM) droplets within the liquid crystal elastomer matrix. Along with the introduction of electrical properties, the inclusion of LM droplets improves thermal conductivity without sacrificing the LCE's mechanical and actuation properties. The coupling of the two materials yields LCE composites with a controlled Joule-heating response and emerging properties of sensing and damage response that can prove useful in artificial muscle applications.³⁴

Efficiency is vital in the discussion of designing artificial muscles. Ambiently heated LCEs exhibit low efficiencies as heat easily dissipates from the actuator into the surrounding tissues.

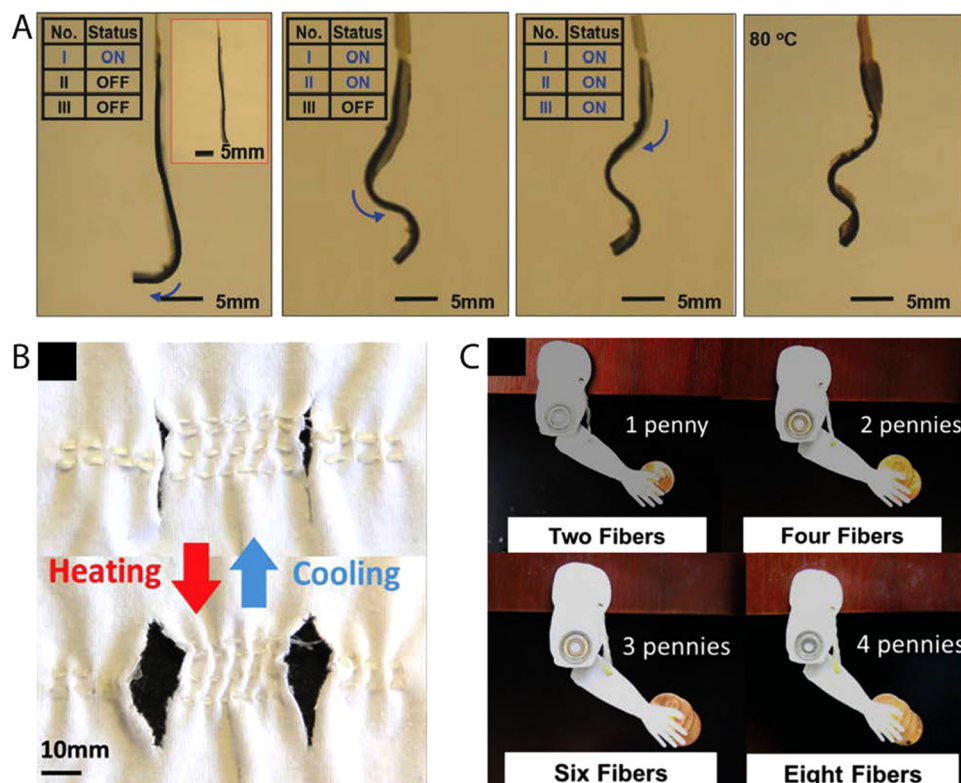


FIG. 8. (a) Selective shape construction of LCE-CB composite via electrical stimulation: sequential snapshots of programmed shapes upon activating heater I (first image), heaters I and II (second image), all the three heaters (third image) for constructing an “S” shape, and a final “S” shape constructed after uniformly heating to 80°C (fourth image). Reproduced with permission from Wang *et al.*, *Adv. Mater.* **30**, 1706695 (2018). Copyright 2018 Wiley. (b) Demonstration of LCE fiber acting as a bicep muscle fiber lifting weight via contracting in response to heat. Snapshots show an increased activation force generated by combining multiple fibers without sacrificing the number of pennies. (c) LCE fibers woven into a fabric with pores. LCE fibers change pore size in the fabric upon heating and cooling. Reproduced with permission from Roach *et al.*, *ACS Appl. Mater. Interfaces* **11**, 19514 (2019). Copyright 2019 American Chemical Society.

A voltage-powered dielectric liquid crystal elastomer actuator (DLCEA) is designed to not only improve efficiency but increase actuation speed compared to ambiently heated LCEs. The DLCEA is fabricated utilizing surface-alignment techniques and thiol-acrylate chemistry.¹⁰⁶ Contrary to most LCEs described in this Perspective, the DLCEA operates where the controlled actuation response occurs perpendicular to the director. Although actuation mode varies, shape-change is still controlled and directed by the alignment imparted within the LCE during surface alignment processing. This specific actuator is able of lifting loads 700 times its mass at strain rates of 120%/s and energy conversion of 20%. Improved actuation speeds and efficiencies of LCE actuators can reinforce their implementation within biomedical device designs.

For LCE actuators to be fully integrated as artificial muscles, they must provide the necessary work to induce movement of the patient's musculoskeletal system or displace necessary loads. Achieving improvement of stress and force output of LCE actuators has been explored in both chemistry and processing developments. Influencing the molecular network of the LCE structure can enhance the stress output of devices made of these materials. Interpenetrating polymer networks of LC polyacrylate, main chain polyurethane, and mesogen LCE produces the highest mechanical properties. A mechanically strained strip comprised of this interpenetrating network can achieve a work capacity of 1267 kJ/m³, up to 86% strain, and 10.4 MPa elastic modulus. These LCEs exhibit comparable strains and elastic moduli to skeletal muscle (40% and 10 MPa–60 MPa).¹⁰⁷ Although shape-change complexity is limited to only stretching and contracting, these LCEs exhibit remarkable and robust actuator properties.

Development of thicker, more complex LCE actuators leads to increased stress and work outputs. Laminated surface-aligned LCEs is one approach to achieve this outcome. LCE films with thickness reaching up to 320 μm fabricated via laminating surface aligned films improved work capacity from 2.6 J/kg to 19 J/kg, while still maintaining complex actuation modes. The LCE laminate can maintain its conical shape in pressures of up to 7 kPa.⁵⁴ This result suggests that LCEs may be used to deform soft tissues. Through 4D printing, LCE structures and fibers can be fabricated on larger size scales, where the minimum thickness is regulated by the nozzle (most instances 300 μm). 4D printed uniaxial actuators that are 1 mm thick are capable of around 43% contraction and could produce a maximum work capacity of 39 J/kg.¹⁴ Printed LCE fibers woven together can lift a mass of up to 250% larger than their mass in response to change in temperature [Fig. 8(b)]. Through weaving these LCE fiber actuators within clothing fabrics, LCEs can be utilized as smart textiles in wearable technologies. When the body's temperature increases, the fibers contract generating pores to allow for heat transfer and increase sweat evaporation [Fig. 8(c)].¹⁰⁸ With 4D printing capabilities, larger and complex LCE actuators can be realized to maximize the work capacity necessary for artificial muscle designs that might be able to function in active prostheses or orthoses.

IV. OUTLOOK

Artificial muscles have been proposed to serve as active components in prosthetic limbs, artificial heart assist devices, and

artificial sphincters.^{109,110} Traditionally, this shape change has been achieved through the engineering of structures with pumps or motors resulting in complex, difficult to operate, or power-demanding systems, which has limited the utility of these machines in clinical practice. Materials that change shape have long been promised to replace some of these systems. For example, shape memory alloys can be powered by Joule heating to undergo high stress and low strain deformation.¹¹¹ These alloys have an elastic modulus greater than six orders of magnitude over soft tissue and undergo strains that are far smaller than natural muscle. Hydrogels can undergo large dimensional changes and have low elastic moduli, but these materials are only capable of exerting small stresses.^{68,112,113} By contrast, LCEs are excellent candidates to serve as artificial muscles due to their large, reversible shape change, low elastic modulus, and moderate stress output.^{30,32,33,42} Several barriers have traditionally limited this interesting class of materials from being used in implanted medical devices: (1) the actuation stress of these materials was low, necessitating large devices to produce moderate forces, (2) the biocompatibility of these materials was unknown, and (3) the temperature required for shape change was incompatible with human tissues. Recent progress in the synthesis, characterization, and processing of LCEs suggests that these barriers can be overcome.^{4,7,95,100,114} In our opinion, applications where the actuator could reversibly deform soft tissues are the most likely to be suitable for LCEs.

One such application is in the treatment of stress urinary incontinence (SUI). SUI is a prevalent condition in women, leading to reduction in quality of life as well as significant annual costs (\$32 billion in the USA/yearly).¹¹⁵ SUI in females arises from a loss of support for the urethra typically provided by the anterior vaginal wall and its lateral attachments to the endopelvic fascia. As these supporting tissues weaken through aging or giving birth, the closing pressure of the urethra decreases, and stress events (e.g., coughing, sneezing) lead to sudden urine loss (incontinence). The surgical management of SUI has been dominated by the sling procedure, especially since the advent of the sub-urethral synthetic slings over the past decades.¹¹⁶ Current slings, either made of autologous tissue or synthetic materials, are placed underneath the urethra to correct urinary incontinence, but these implants behave like a permanent fixture that does not adapt to voiding mechanics or continence needs.^{117–119} The sling is in place forever and fixated in scar tissue. LCEs may enable opportunities to fundamentally alter this approach. Successful devices will require that (1) the amplitude of the deformation and force and response time must be sufficient to replace the function of the native tissue, (2) the device must be powered in a way that does not harm surrounding tissue, and (3) the device should deform repeatedly for thousands (or more) of cycles in physiological conditions. We envision the use of carbon black-LCE slings that provide support to the urethra, enabling continence (Fig. 9). Through combining carbon black's photo-thermal property and 2-click thiol-acrylate and thiol-ene chemistry's tunable transition temperatures, we 4D print a low-temperature, IR responsive LCE sling. DIW printing allows for control over the director orientation within the composite sling and patient specificity. We previously reported a 4D printable composition that exhibits a glass transition temperature

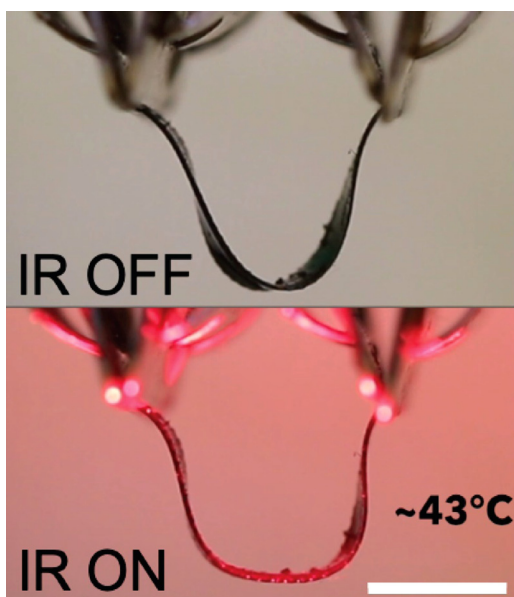


FIG. 9. Snapshots of NIR light responsive CB-LCE composite actuating in air. A CB-LCE sling in a “U” shape, mimicking the mechanism by which mesh slings for stress urinary incontinence support urethra (top). CB-LCE sling widens its radius of curvature after the application of 300 mW/cm^2 NIR light for 30 s at a 15 mm distance and reaching a temperature of $43 \text{ }^\circ\text{C}$ (bottom). Scale bar: 5 mm.

around $-10 \text{ }^\circ\text{C}$, and an elastic modulus of $\sim 8 \text{ MPa}$ near room temperature. When heated, the elastic modulus drops to 1 MPa . Actuation of this composition begins around $35 \text{ }^\circ\text{C}$ and about 10% actuation strain is observed on heating to $50 \text{ }^\circ\text{C}$.²³ Due to these properties, we believe that this composition may be appropriate for some medical devices that undergo reversible shape change. To enable photo-controlled actuation of this material, carbon black was mixed with a RM82-EDDT-TATATO composition to form an oligomer ink. LC phase properties are not changed with the inclusion of carbon black as evident by differential scanning calorimetry thermographs exhibiting no change in T_{NI} (Fig. S1). We expect that the inclusion of carbon black should not drastically alter the mechanical properties and actuation behavior. The LCE ink is extruded and photocrosslinked with the director along the short axis of the sling. As demonstrated in Fig. 9, the LCE composite sling would be applied around the urethra for support. On application of near-IR light, the sling would be heated photothermally through the skin. Near-IR light is capable of transmitting through the skin and will be absorbed by the carbon black LCE composite. The director design allows for elongation perpendicular to the urethra on heating leading to a relaxation of support. After about 3 min at tolerable heating levels ($43 \text{ }^\circ\text{C}$) would provoke a shape-change allowing the patient to void with ease on command. Due to the reversible shape-changing behavior of LCEs, the sling would contract and provide the necessary urethra support when the

stimulus disappears. This concept is enabled by recent advances in tuning the transition temperature of LCEs prepared through DIW printing. We note that thermal stimulation of tissue has already been utilized within commercially available treatments. Heating pads used for tissue relaxation commonly reach temperatures of above $45 \text{ }^\circ\text{C}$, and ThermoDox, an FDA-approved drug therapy, utilizes thermal stimulation up to $45 \text{ }^\circ\text{C}$ to treat tumor cells. Significant questions remain about the stability of these materials in a physiological environment, and the tissue responses to heat and shape change. We are currently exploring this proposed LCE system.

V. CONCLUSION

Within this review, we cover the processing advances that have allowed major advances in the field of LCEs. After reviewing the main developments of this field, we venture into the application of LCE in the field of biomedical devices to illustrate their newer roles and growth potential. The emergence of potential biomedical applications is a result of the vast chemistries and processing strategies to fabricate LCEs. The potential for LCE application is, in large part, dictated by advances in the alignment processes used to control the shape change of these materials. The decoupling of the alignment and crosslinking steps associated with mechanical straining strategies allow for robust uniaxial actuators. This strategy enables facile processing of electro-thermally responsive, composite LCE actuators for potential future wearable orthoses. Surface aligned LCEs allow for high resolution control over the alignment director of thin films. The hierarchical control enables highly complex shape-change, such as cones and helices. By taking advantage of alignment control and lithography compatibility, surface aligned strategies enable design of 3D substrates that are promising substrates for stretchable electronics. 4D printing processes have enabled the development of low-temperature and light-responsive LCE structures. As elaborated within the outlook, a light-responsive, low-temperature implantable dynamic sling is in development to potentially treat urinary incontinence. Further understanding of the relationships between LCE chemistry and processing is vital for the realization of future LCE applications. With the expansion of processing techniques and strategies, LCEs are poised to make a significant impact in the field of biomedical devices.

VI. METHODS

A. Carbon black-LCE sling fabrication

The composite ink is prepared by mixing diacrylate mesogen 1,4-bis-[4-(6-acryloyloxyhexyloxy)benzoyloxy]-2-methylbenzene (RM82), dithiol spacer 2,2'-(ethylenedioxy) diethanethiol (EDDT), and vinyl crosslinker 1,3,5-triallyl-1,3,5-triazine-2,4,6-(1H,3H,5H)-trione (TATATO) in a 0.8:1.0:0.2 molar ratio with 0.2 wt. % of carbon black, 1 wt. % triethylamine, 1 wt. % BHT, and 3.5 wt. % I-369 in a glass vial. The monomer precursors are mixed with heat until homogeneous. The solution is transferred to a syringe and allowed to oligomerize at $65 \text{ }^\circ\text{C}$ for 3 h. Upon completion of oligomerization, the LCE ink is ready for printing. The printing conditions of the material are a needle size of 24 G,

printing speeds of 2 mm s^{-1} , printing temperature of $38 \text{ }^\circ\text{C}$, and irradiation intensity of 0.8 mW cm^{-2} from 365 nm LEDs. The printed samples are then cured under 365 nm UV light for 20 min .

SUPPLEMENTARY MATERIAL

See the [supplementary material](#) for the DSC thermogram of the 2-click thiol–acrylate and thiol–ene chemistry with and without carbon black concentrations in Fig. S1. There is no change in T_{NI} between the control LCE compositions and the $0.2 \text{ wt. } \%$ CB–LCE. The addition of carbon black does not alter the liquid crystalline phase properties of the printable LC ink.

ACKNOWLEDGMENTS

This material is partially based upon work supported by the National Science Foundation (NSF) under Grant No. DMR-1752846. Research reported in this publication was partially supported by the National Institute of Biomedical Imaging and Bioengineering of the National Institutes of Health under Award No. R21EB028547. The content is solely the responsibility of the authors and does not necessarily represent the official views of the National Institutes of Health. This material was partially based upon the work supported by the Air Force Office of Scientific Research under Award No. FA9550-17-1-0328.

DATA AVAILABILITY

The data that support the findings of this study are available from the corresponding author upon reasonable request.

REFERENCES

- ¹P. J. Collings and J. W. Goodby, *Introduction to Liquid Crystals: Chemistry and Physics* (CRC Press, 2019).
- ²P. G. De Gennes, *CR Acad. Sci. Ser. B* **281**, 101 (1975).
- ³H. Wermter and H. Finkelmann, *E-Polymers* **1**, 111 (2001).
- ⁴C. M. Yakacki, M. Saed, D. P. Nair, T. Gong, S. M. Reed, and C. N. Bowman, *RSC Adv.* **5**, 18997 (2015).
- ⁵Y. Yao, J. T. Waters, A. V. Shneidman, J. Cui, X. Wang, N. K. Mandsberg, S. Li, A. C. Balazs, and J. Aizenberg, *Proc. Natl. Acad. Sci. U.S.A.* **115**, 12950 (2018).
- ⁶T. H. Ware, M. E. McConney, J. J. Wie, V. P. Tondiglia, and T. J. White, *Science* **347**, 982 (2015).
- ⁷C. P. Ambulo, J. J. Burroughs, J. M. Boothby, H. Kim, M. R. Shankar, and T. H. Ware, *ACS Appl. Mater. Interfaces* **9**, 37332 (2017).
- ⁸P. Beyer, E. M. Terentjev, and R. Zentel, *Macromol. Rapid Commun.* **28**, 1485 (2007).
- ⁹S. Krause, R. Dersch, J. H. Wendorff, and H. Finkelmann, *Macromol. Rapid Commun.* **28**, 2062 (2007).
- ¹⁰H. Yang, A. Buguin, J.-M. Taulemesse, K. Kaneko, S. Méry, A. Bergeret, and P. Keller, *J. Am. Chem. Soc.* **131**, 15000 (2009).
- ¹¹Y. Xia, G. Cedillo-Servin, R. D. Kamien, and S. Yang, *Adv. Mater.* **28**, 9637 (2016).
- ¹²H. Zeng, O. M. Wani, P. Wasylczyk, R. Kaczmarek, and A. Priimagi, *Adv. Mater.* **29**, 1701814 (2017).
- ¹³M. López-Valdeolivas, D. Liu, D. J. Broer, and C. Sánchez-Somolinos, *Macromol. Rapid Commun.* **39**, 1700710 (2018).
- ¹⁴A. Kotikian, R. L. Truby, J. W. Boley, T. J. White, and J. A. Lewis, *Adv. Mater.* **30**, 1706164 (2018).
- ¹⁵M. Barnes and R. Verduzco, *Soft Matter* **15**, 870 (2019).
- ¹⁶S. Schuhladen, F. Preller, R. Rix, S. Petsch, R. Zentel, and H. Zappe, *Adv. Mater.* **26**, 7247 (2014).
- ¹⁷M. O. Saed, A. H. Torbati, C. A. Starr, R. Visvanathan, N. A. Clark, and C. M. Yakacki, *J. Polym. Sci. Part B Polym. Phys.* **55**, 157 (2017).
- ¹⁸Q. Zhang, X. Kuang, S. Weng, Z. Zhao, H. Chen, D. Fang, and H. J. Qi, *ACS Appl. Mater. Interfaces* **12**, 17979 (2020).
- ¹⁹X. Qian, Q. Chen, Y. Yang, Y. Xu, Z. Li, Z. Wang, Y. Wu, Y. Wei, and Y. Ji, *Adv. Mater.* **30**, 1801103 (2018).
- ²⁰X. Liu, R. Wei, P. T. Hoang, X. Wang, T. Liu, and P. Keller, *Adv. Funct. Mater.* **25**, 3022 (2015).
- ²¹N. P. Godman, B. A. Kowalski, A. D. Auguste, H. Koerner, and T. J. White, *ACS Macro Lett.* **6**, 1290 (2017).
- ²²H. Zeng, D. Martella, P. Wasylczyk, G. Cerretti, J. G. Lavocat, C. Ho, C. Parmeggiani, and D. S. Wiersma, *Adv. Mater.* **26**, 2319 (2014).
- ²³M. O. Saed, C. P. Ambulo, H. Kim, R. De, V. Raval, K. Searles, D. A. Siddiqui, J. M. O. Cue, M. C. Stefan, M. R. Shankar, and T. H. Ware, *Adv. Funct. Mater.* **29**, 1806412 (2018).
- ²⁴M. Tabrizi, T. H. Ware, and M. R. Shankar, *ACS Appl. Mater. Interfaces* **11**, 28236 (2019).
- ²⁵R. H. Volpe, D. Mistry, V. V. Patel, R. R. Patel, and C. M. Yakacki, *Adv. Healthc. Mater.* **9**, 1901136 (2020).
- ²⁶D. R. Merkel, N. A. Traugutt, R. Visvanathan, C. M. Yakacki, and C. P. Frick, *Soft Matter* **14**, 6024 (2018).
- ²⁷D. W. Hanzon, N. A. Traugutt, M. K. McBride, C. N. Bowman, C. M. Yakacki, and K. Yu, *Soft Matter* **14**, 951 (2018).
- ²⁸H. Finkelmann, H. Kock, W. Gleim, and G. Rehage, *Die Makromol. Chem. Rapid Commun.* **5**, 287 (1984).
- ²⁹B. Donnio, H. Wermter, and H. Finkelmann, *Macromolecules* **33**, 7724 (2000).
- ³⁰J. K pfer and H. Finkelmann, *Die Makromol. Chem. Rapid Commun.* **12**, 717 (1991).
- ³¹Y. Xia, X. Zhang, and S. Yang, *Angew. Chem.* **130**, 5767 (2018).
- ³²Z. Pei, Y. Yang, Q. Chen, E. M. Terentjev, Y. Wei, and Y. Ji, *Nat. Mater.* **13**, 36 (2014).
- ³³A. Agrawal, H. Chen, H. Kim, B. Zhu, O. Adetiba, A. Miranda, A. Cristian Chipara, P. M. Ajayan, J. G. Jacot, and R. Verduzco, *ACS Macro Lett.* **5**, 1386 (2016).
- ³⁴M. J. Ford, C. P. Ambulo, T. A. Kent, E. J. Markvicka, C. Pan, J. Malen, T. H. Ware, and C. Majidi, *Proc. Natl. Acad. Sci. U.S.A.* **116**, 21438 (2019).
- ³⁵S. Banisadr and J. Chen, *Sci. Rep.* **7**, 1 (2017).
- ³⁶R. S. Kularatne, H. Kim, J. M. Boothby, and T. H. Ware, *J. Polym. Sci. Part B Polym. Phys.* **55**, 395 (2017).
- ³⁷M. Wang, S. M. Sayed, L.-X. Guo, B.-P. Lin, X.-Q. Zhang, Y. Sun, and H. Yang, *Macromolecules* **49**, 663 (2016).
- ³⁸C. Wang, K. Sim, J. Chen, H. Kim, Z. Rao, Y. Li, W. Chen, J. Song, R. Verduzco, and C. Yu, *Adv. Mater.* **30**, 1706695 (2018).
- ³⁹H. Xing, J. Li, Y. Shi, J. Guo, and J. Wei, *ACS Appl. Mater. Interfaces* **8**, 9440 (2016).
- ⁴⁰W. H. De Jeu, *Liquid Crystal Elastomers: Materials and Applications* (Springer, 2012).
- ⁴¹F. Ge and Y. Zhao, *Adv. Funct. Mater.* **30**, 1901890 (2020).
- ⁴²A. Buguin, M. H. Li, P. Silberzan, B. Ladoux, and P. Keller, *J. Am. Chem. Soc.* **128**, 1088 (2006).
- ⁴³J. T. Waters, S. Li, Y. Yao, M. M. Lerch, M. Aizenberg, J. Aizenberg, and A. C. Balazs, *Sci. Adv.* **6**, eaay5349 (2020).
- ⁴⁴S. Y. Yang, E. D. O’Cearbhaill, G. C. Sisk, K. M. Park, W. K. Cho, M. Villiger, B. E. Bouma, B. Pomahac, and J. M. Karp, *Nat. Commun.* **4**, 1702 (2013).
- ⁴⁵X. Zhao, J. Kim, C. A. Cezar, N. Huebsch, K. Lee, K. Bouhadir, and D. J. Mooney, *Proc. Natl. Acad. Sci. U.S.A.* **108**, 67 (2011).
- ⁴⁶Y. Sapir, S. Cohen, G. Friedman, and B. Polyak, *Biomaterials* **33**, 4100 (2012).

- ⁴⁷M. Schadt, K. Schmitt, V. Kozinkov, and V. Chigrinov, *Jpn. J. Appl. Phys.* **31**, 2155 (1992).
- ⁴⁸K. Ichimura, *Chem. Rev.* **100**, 1847 (2000).
- ⁴⁹B. Jerome, *Rep. Prog. Phys.* **54**, 391 (1991).
- ⁵⁰S. W. Ula, N. A. Traugott, R. H. Volpe, R. R. Patel, K. Yu, and C. M. Yakacki, *Liq. Cryst. Rev.* **6**, 78 (2018).
- ⁵¹H. Shahsavan, S. M. Salili, A. Jáklí, and B. Zhao, *Adv. Mater.* **27**, 6828 (2015).
- ⁵²J. M. Boothby and T. H. Ware, *Soft Matter* **13**, 4349 (2017).
- ⁵³A. D. Auguste, J. W. Ward, J. O. Hardin, B. A. Kowalski, T. C. Guin, J. D. Berrigan, and T. J. White, *Adv. Mater.* **30**, 1802438 (2018).
- ⁵⁴T. Guin, M. J. Settle, B. A. Kowalski, A. D. Auguste, R. V. Beblo, G. W. Reich, and T. J. White, *Nat. Commun.* **9**, 2531 (2018).
- ⁵⁵G. Babakhanova, T. Turiv, Y. Guo, M. Hendrikx, Q.-H. Wei, A. P. H. J. Schenning, D. J. Broer, and O. D. Lavrentovich, *Nat. Commun.* **9**, 456 (2018).
- ⁵⁶R. A. M. Hikmet and D. J. Broer, *Polymer* **32**, 1627 (1991).
- ⁵⁷T. H. Ware, Z. P. Perry, C. M. Middleton, S. T. Iacono, and T. J. White, *ACS Macro Lett.* **4**, 942 (2015).
- ⁵⁸D. L. Thomsen, P. Keller, J. Naciri, R. Pink, H. Jeon, D. Shenoy, and B. R. Ratna, *Macromolecules* **34**, 5868 (2001).
- ⁵⁹J. M. McCracken, V. P. Tondiglia, A. D. Auguste, N. P. Godman, B. R. Donovan, B. N. Bagnall, H. E. Fowler, C. M. Baxter, V. Matavulj, J. D. Berrigan, and T. J. White, *Adv. Funct. Mater.* **29**, 1903761 (2019).
- ⁶⁰H.-H. Yoon, D.-Y. Kim, K.-U. Jeong, and S. Ahn, *Macromolecules* **51**, 1141 (2018).
- ⁶¹S. Ahn, T. H. Ware, K. M. Lee, V. P. Tondiglia, and T. J. White, *Adv. Funct. Mater.* **26**, 5819 (2016).
- ⁶²H. Shahsavan, A. Aghakhani, H. Zeng, Y. Guo, Z. S. Davidson, A. Priimagi, and M. Sitti, *Proc. Natl. Acad. Sci. U.S.A.* **117**, 5125 (2020).
- ⁶³Y. Cheng, H. Lu, X. Lee, H. Zeng, and A. Priimagi, *Adv. Mater.* **32**, 1906233 (2020).
- ⁶⁴H. Zeng, O. M. Wani, P. Wasylczyk, and A. Priimagi, *Macromol. Rapid Commun.* **39**, 1700224 (2018).
- ⁶⁵Y. Y. C. Choong, S. Maleksaedi, H. Eng, J. Wei, and P.-C. Su, *Mater. Des.* **126**, 219 (2017).
- ⁶⁶M. Zarek, N. Mansour, S. Shapira, and D. Cohn, *Macromol. Rapid Commun.* **38**, 1600628 (2016).
- ⁶⁷Q. Ge, A. H. Sakhaei, H. Lee, C. K. Dunn, N. X. Fang, and M. L. Dunn, *Sci. Rep.* **6**, 31110 (2016).
- ⁶⁸A. Sydney Gladman, E. A. Matsumoto, R. G. Nuzzo, L. Mahadevan, and J. A. Lewis, *Nat. Mater.* **15**, 413 (2016).
- ⁶⁹C. D. Modes and M. Warner, *Europhys. Lett.* **97**, 36007 (2012).
- ⁷⁰D. J. Roach, X. Kuang, C. Yuan, K. Chen, and H. J. Qi, *Smart Mater. Struct.* **27**, 125011 (2018).
- ⁷¹J. E. Huber, N. A. Fleck, and M. F. Ashby, *Proc. R. Soc. Lond. Ser. A Math. Phys. Eng. Sci.* **453**, 2185 (1997).
- ⁷²S. Chéry-Croze, *Pain* **17**, 109 (1983).
- ⁷³A. Kotikian, C. McMahan, E. C. Davidson, J. M. Muhammad, R. D. Weeks, C. Daraio, and J. A. Lewis, *Sci. Robot.* **4**, eaax7044 (2019).
- ⁷⁴E. C. Davidson, A. Kotikian, S. Li, J. Aizenberg, and J. A. Lewis, *Adv. Mater.* **32**, 1905682 (2020).
- ⁷⁵R. A. M. Hikmet, *J. Appl. Phys.* **68**, 4406 (1990).
- ⁷⁶D. J. Broer, J. Lub, and G. N. Mol, *Nature* **378**, 467 (1995).
- ⁷⁷T. Ikeda and O. Tsutsumi, *Science* **268**, 1873 (1995).
- ⁷⁸J. Lub, D. J. Broer, R. A. M. Hikmet, and K. G. J. Nierop, *Liq. Cryst.* **18**, 319 (1995).
- ⁷⁹D. Liu and D. J. Broer, *Angew. Chem.* **126**, 4630 (2014).
- ⁸⁰D. J. Mulder, A. Schenning, and C. W. M. Bastiaansen, *J. Mater. Chem. C* **2**, 6695 (2014).
- ⁸¹T. J. White and D. J. Broer, *Nat. Mater.* **14**, 1087 (2015).
- ⁸²S. Gantenbein, K. Masania, W. Woigk, J. P. W. Sesse, T. A. Tervoort, and A. R. Studart, *Nature* **561**, 226 (2018).
- ⁸³R. S. Kularatne, H. Kim, M. Ammanamanchi, H. N. Hayenga, and T. H. Ware, *Chem. Mater.* **28**, 8489 (2016).
- ⁸⁴J. M. Boothby, J. Samuel, and T. H. Ware, *Soft Matter* **15**, 4508 (2019).
- ⁸⁵D. R. Merkel, R. K. Shaha, C. M. Yakacki, and C. P. Frick, *Polymer* **166**, 148 (2019).
- ⁸⁶R. K. Shaha, D. R. Merkel, M. P. Anderson, E. J. Devreux, R. R. Patel, A. H. Torbati, N. Willett, C. M. Yakacki, and C. P. Frick, *J. Mech. Behav. Biomed. Mater.* **107**, 103757 (2020).
- ⁸⁷H. Aubin, J. W. Nichol, C. B. Hutson, H. Bae, A. L. Sieminski, D. M. Crokek, P. Akhyari, and A. Khademhosseini, *Biomaterials* **31**, 6941 (2010).
- ⁸⁸D. Martella and C. Parmeggiani, *Chem. Eur. J.* **24**, 12206 (2018).
- ⁸⁹G. Babakhanova, J. Krieger, B. Li, T. Turiv, M. Kim, and O. D. Lavrentovich, *J. Biomed. Mater. Res. Part A* **108**, 1223 (2020).
- ⁹⁰T. Turiv, J. Krieger, G. Babakhanova, H. Yu, S. V. Shiyanski, Q.-H. Wei, M.-H. Kim, and O. D. Lavrentovich, *Sci. Adv.* **6**, eaaz6485 (2020).
- ⁹¹C. T. Lim, E. H. Zhou, and S. T. Quek, *J. Biomech.* **39**, 195 (2006).
- ⁹²R. Edmondson, J. J. Broglie, A. F. Adcock, and L. Yang, *Assay Drug Dev. Technol.* **12**, 207 (2014).
- ⁹³Y. Pang, X. Wang, D. Lee, and H. P. Greisler, *Biomaterials* **32**, 3776 (2011).
- ⁹⁴M. Prévôt and E. Hegmann, *Advances in Bioinspired Biomedical Materials* (ACS Publications, 2017), Vol. 2.
- ⁹⁵T. Bera, E. J. Freeman, J. A. McDonough, R. J. Clements, A. Aladlaan, D. W. Miller, C. Malcuit, T. Hegmann, and E. Hegmann, *ACS Appl. Mater. Interfaces* **7**, 14528 (2015).
- ⁹⁶Y. Gao, T. Mori, S. Manning, Y. Zhao, A. D. Nielsen, A. Neshat, A. Sharma, C. J. Mahnen, H. R. Everson, S. Crotty, R. J. Clements, C. Malcuit, and E. Hegmann, *ACS Macro Lett.* **5**, 4 (2016).
- ⁹⁷T. Mori, R. Cukelj, M. E. Prévôt, S. Ustunel, A. Story, Y. Gao, K. Diabre, J. A. McDonough, E. J. Freeman, E. Hegmann, and R. J. Clements, *Macromol. Rapid Commun.* **41**, 1900585 (2020).
- ⁹⁸H. Kim, J. Gibson, J. Maeng, M. O. Saed, K. Pimentel, R. T. Rihani, J. J. Pancrazio, S. V. Georgakopoulos, and T. H. Ware, *ACS Appl. Mater. Interfaces* **11**, 19506 (2019).
- ⁹⁹J. Maeng, R. T. Rihani, M. Javed, J. S. Rajput, H. Kim, I. G. Bouton, T. A. Criss, J. J. Pancrazio, B. J. Black, and T. H. Ware, *J. Mater. Chem. B* **8**, 6286 (2020).
- ¹⁰⁰R. T. Rihani, H. Kim, B. J. Black, R. Atmaramani, M. O. Saed, J. J. Pancrazio, and T. H. Ware, *Micromachines* **9**, 416 (2018).
- ¹⁰¹H. Kim, J. A. Lee, C. P. Ambulo, H. B. Lee, S. H. Kim, V. V. Naik, C. S. Haines, A. E. Aliev, R. Ovalle-Robles, R. H. Baughman, and T. H. Ware, *Adv. Funct. Mater.* **29**, 1905063 (2019).
- ¹⁰²Z. Wang, K. Li, Q. He, and S. Cai, *Adv. Mater.* **31**, 1806849 (2018).
- ¹⁰³C. Ferrantini, J. M. Pioner, D. Martella, R. Coppini, N. Piroddi, P. Paoli, M. Calamai, F. S. Pavone, D. S. Wiersma, C. Tesi, E. Cerbai, C. Poggesi, L. Sacconi, and C. Parmeggiani, *Circ. Res.* **124**, e44 (2019).
- ¹⁰⁴T. Guin, H. E. Hinton, E. Burgeson, C. C. Bowland, L. T. Kearney, L. Yuhzan, I. Ivanov, N. A. Nguyen, and A. K. Naskar, *Adv. Intell. Syst.* **2**, 2000022 (2020).
- ¹⁰⁵Q. He, Z. Wang, Y. Wang, A. Minori, M. T. Tolley, and S. Cai, *Sci. Adv.* **5**, eaax5746 (2019).
- ¹⁰⁶Z. S. Davidson, H. Shahsavan, A. Aghakhani, Y. Guo, L. Hines, Y. Xia, S. Yang, and M. Sitti, *Sci. Adv.* **5**, eaay0855 (2019).
- ¹⁰⁷H.-F. Lu, M. Wang, X.-M. Chen, B.-P. Lin, and H. Yang, *J. Am. Chem. Soc.* **141**, 14364 (2019).
- ¹⁰⁸D. J. Roach, C. Yuan, X. Kuang, V. C.-F. Li, P. Blake, M. L. Romero, I. Hammel, K. Yu, and H. J. Qi, *ACS Appl. Mater. Interfaces* **11**, 19514 (2019).
- ¹⁰⁹E. Smela, *Adv. Mater.* **15**, 481 (2003).
- ¹¹⁰E. T. Roche, M. A. Horvath, I. Wamala, A. Alazmani, S.-E. Song, W. Whyte, Z. Machaidze, C. J. Payne, J. C. Weaver, G. Fishbein, J. Kuebler, N. V. Vasilyev, D. J. Mooney, F. A. Pigula, and C. J. Walsh, *Sci. Transl. Med.* **9**, eaaf3925 (2017).

- ¹¹¹F. El Feninat, G. Laroche, M. Fiset, and D. Mantovani, *Adv. Eng. Mater.* **4**, 91 (2002).
- ¹¹²R. L. Truby and J. A. Lewis, *Nature* **540**, 371 (2016).
- ¹¹³S. E. Bakarich, R. Gorkin III, M. In Het Panhuis, and G. M. Spinks, *Macromol. Rapid Commun.* **36**, 1211 (2015).
- ¹¹⁴H. Kim, J. M. Boothby, S. Ramachandran, C. D. Lee, and T. H. Ware, *Macromolecules* **50**, 4267 (2017).
- ¹¹⁵D. Lee and P. E. Zimmern, *EMJ* **1**, 103 (2016).
- ¹¹⁶R. R. Rackley, J. B. Abdelmalak, M. B. Tchegen, S. Madjar, S. Jones, and M. Noble, *Tech. Urol.* **7**, 90 (2001).
- ¹¹⁷C. R. Chapple, S. Raz, L. Brubaker, and P. E. Zimmern, *Eur. Urol.* **64**, 525 (2013).
- ¹¹⁸K. Keltie, S. Elneil, A. Monga, H. Patrick, J. Powell, B. Campbell, and A. J. Sims, *Sci. Rep.* **7**, 12015 (2017).
- ¹¹⁹J. C. Hou, F. Alhalabi, G. E. Lemack, and P. E. Zimmern, *J. Urol.* **192**, 856 (2014).